

INFLUENCE OF MICROSTRUCTURE ON DEBONDING AT THE FIBER/MATRIX INTERFACE IN FIBER-REINFORCED POLYMERS UNDER TENSILE LOADING

Luca Di Stasio^{1,2}

Supervisors: Janis Varna¹, Zoubir Ayadi²

¹Division of Materials Science, Luleå University of Technology, Luleå, Sweden

²EEIGM & IJL, Université de Lorraine, Nancy, France

Luleå (SE) - December 13, 2019



Outline

- ➔ Introduction
- ➔ Modeling
- ➔ Convergence
- ➔ Debond Initiation
- ➔ Debond Propagation
- ➔ Moving Forward

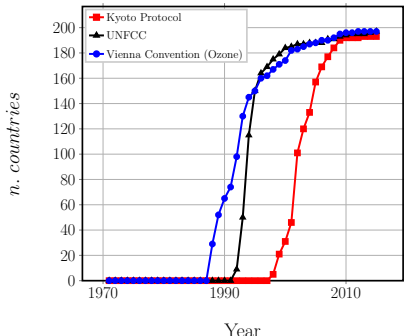
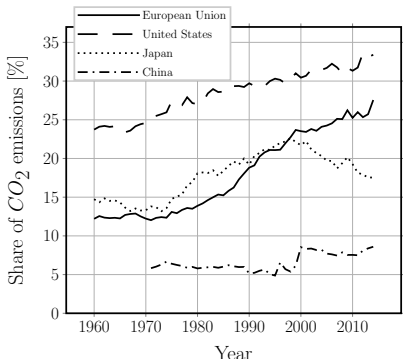
Introduction Modeling Convergence Debond Initiation Debond Propagation Moving Forward

Challenges of the transport sector The Thin-ply "Advantage" Micromechanics of Initiation

INTRODUCTION

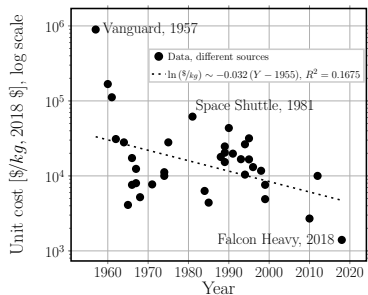
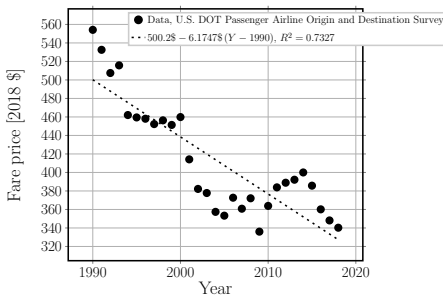
Challenges of the transport sector

- Institutional and popular pressure to reduce CO_2 emissions



Challenges of the transport sector

- Downward pressure on prices

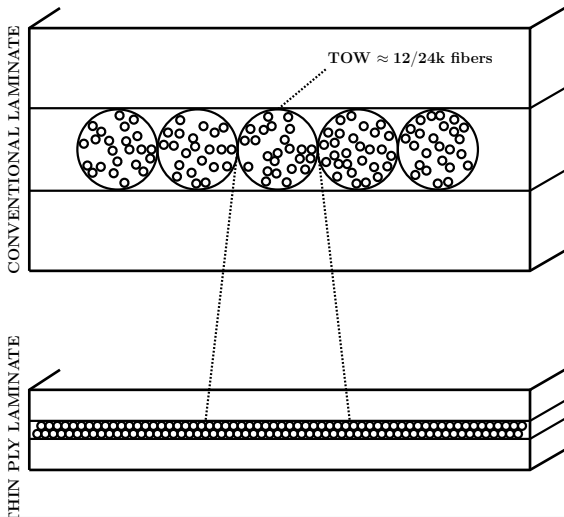


Challenges of the transport sector

- Strict requirements of safety and crashworthiness

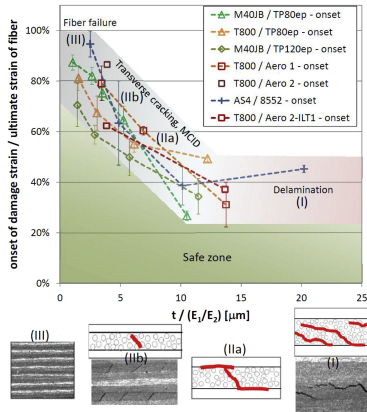


The Thin-ply "Advantage": new material



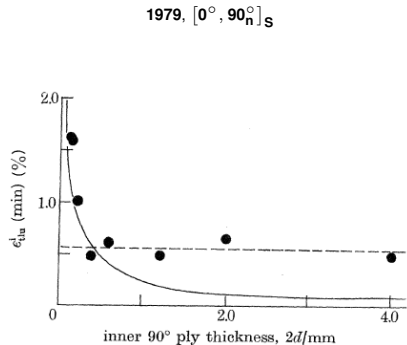
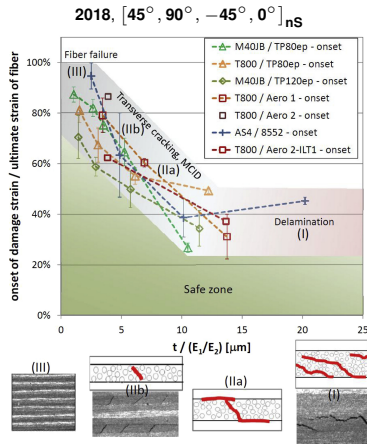
The Thin-ply "Advantage": new material

2018, $[45^\circ, 90^\circ, -45^\circ, 0^\circ]_{ns}$

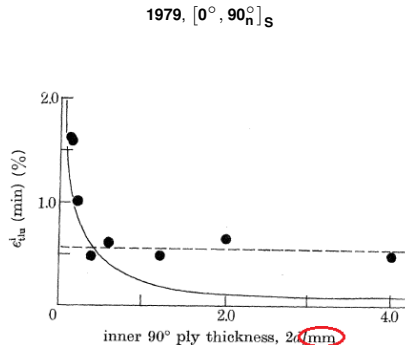
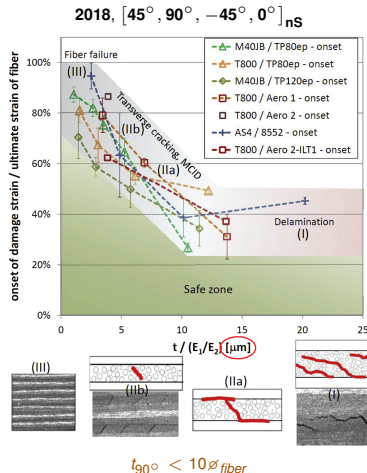


Cugnoni et al., Compos. Sci. Technol. **168**, 2018.

The Thin-ply "Advantage": new material, old result



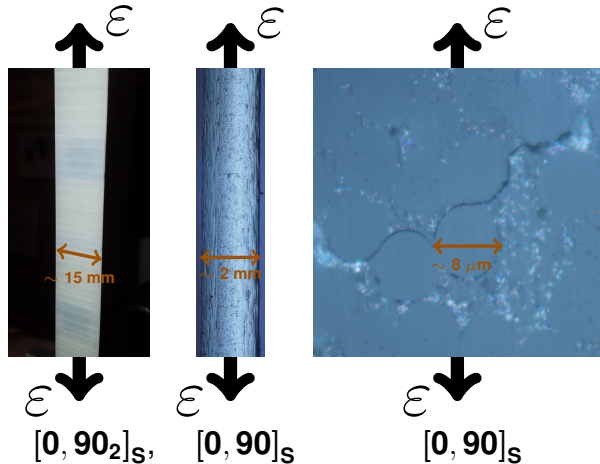
The Thin-ply "Advantage": new material, old result?



Cugnoni et al., Compos. Sci. Technol. **168**, 2018.

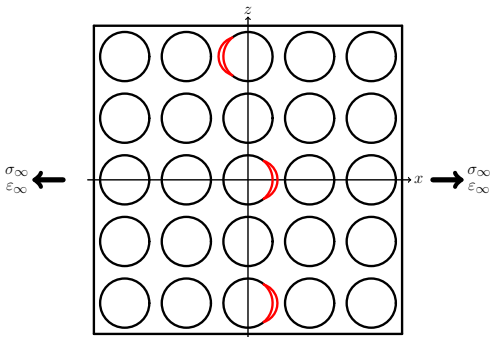
Bailey et al., P. Roy. Soc. A-Math. Phys. **366** (1727), 1979.

Micromechanics of Initiation



Micromechanics of Initiation

Stage 1: isolated debonds



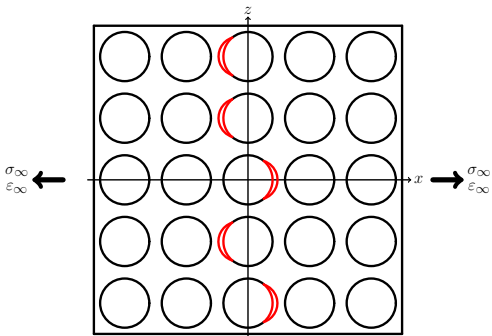
Bailey et al., P. Roy. Soc. A-Math. Phy. **366** (1727), 1979.

Bailey et al., J. Mater. Sci. **16** (3), 1981.

Zhang et al., Compos. Part A-Appl. S. **28** (4), 1997.

Micromechanics of Initiation

Stage 2: consecutive debonds



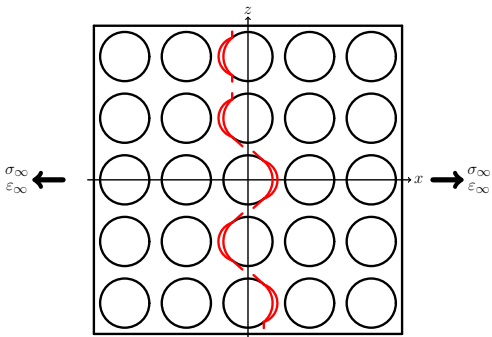
Bailey et al., P. Roy. Soc. A-Math. Phy. **366** (1727), 1979.

Bailey et al., J. Mater. Sci. **16** (3), 1981.

Zhang et al., Compos. Part A-Appl. S. **28** (4), 1997.

Micromechanics of Initiation

Stage 3: kinking



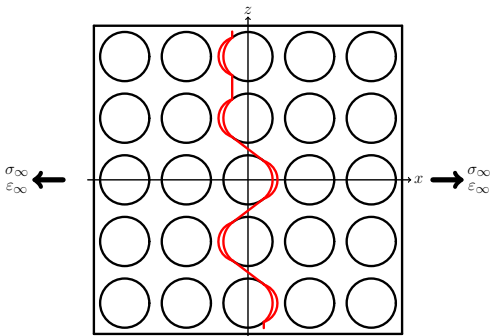
Bailey et al., P. Roy. Soc. A-Math. Phy. **366** (1727), 1979.

Bailey et al., J. Mater. Sci. **16** (3), 1981.

Zhang et al., Compos. Part A-Appl. S. **28** (4), 1997.

Micromechanics of Initiation

Stage 4: coalescence



Bailey et al., P. Roy. Soc. A-Math. Phy. **366** (1727), 1979.

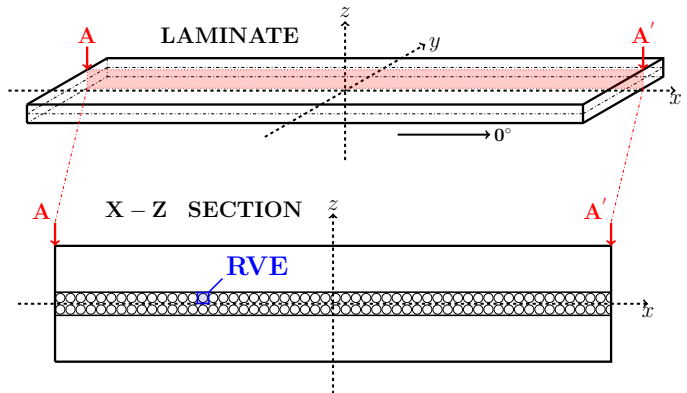
Bailey et al., J. Mater. Sci. **16** (3), 1981.

Zhang et al., Compos. Part A-Appl. S. **28** (4), 1997.

Introduction Modeling Convergence Debond Initiation Debond Propagation Moving Forward
Geometry Representative Volume Elements Equivalent boundary conditions Assumptions Solution

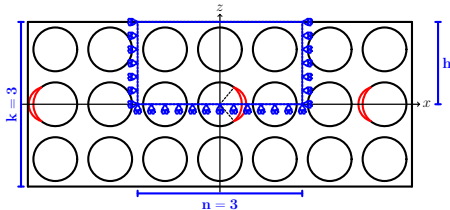
MODELING

Geometry



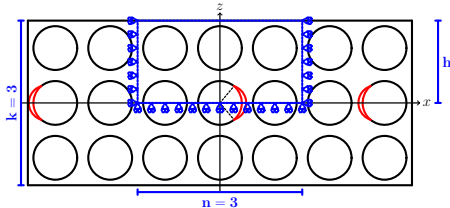
- $L, W \gg t$
- $L, W \rightarrow \infty$
- Square packing
- $L_d \gg \Delta\theta_d$
- 2D RVE

Representative Volume Elements



$n \times k - \text{free}$

Representative Volume Elements

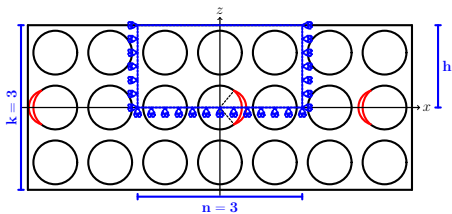


$n \times k - \text{free}$

$n \times k - H$

$$H : u_x(x, h) = \bar{\varepsilon}_x x$$

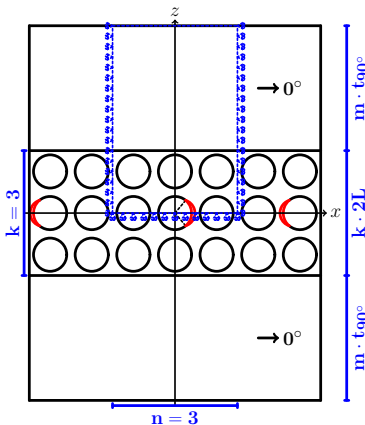
Representative Volume Elements



$n \times k - \text{free}$

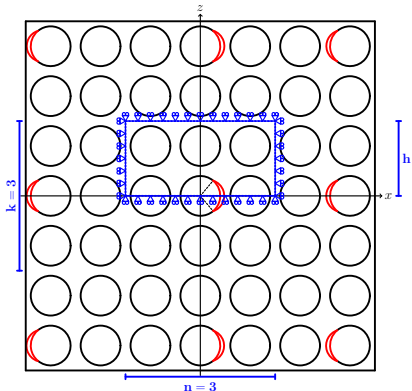
$n \times k - H$

$$H: u_x(x, h) = \bar{\varepsilon}_x x$$



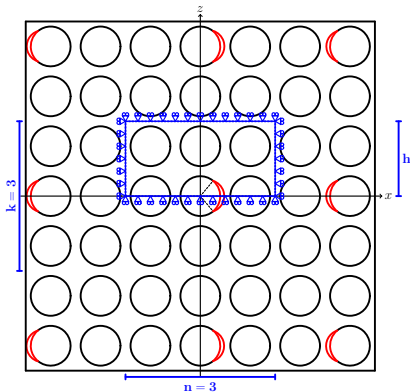
$$n \times k - m \cdot t_{90^\circ}$$

Representative Volume Elements



$n \times k - \text{symm (coupling)}$

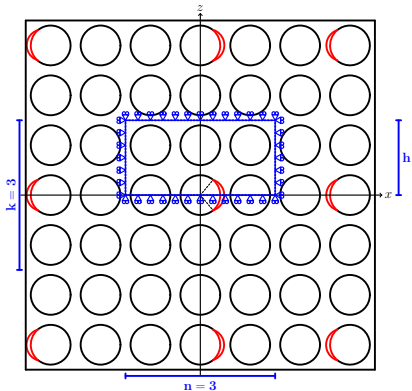
Representative Volume Elements



$n \times k - \text{symm (coupling)}$

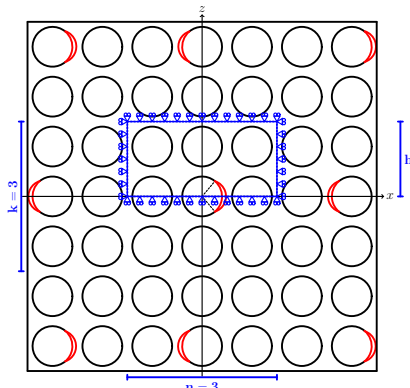
$n \times k - \text{coupling} + H$

Representative Volume Elements



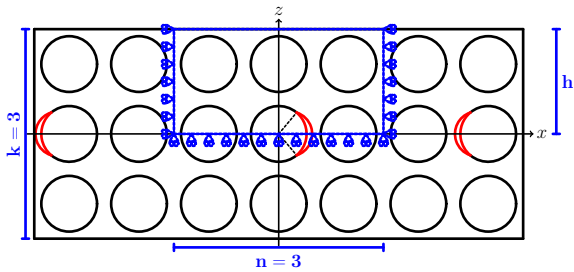
$n \times k - \text{symm (coupling)}$

$n \times k - \text{coupling} + H$



$n \times k - \text{asymm}$

Equivalent boundary conditions: linear horizontal displacement (H)

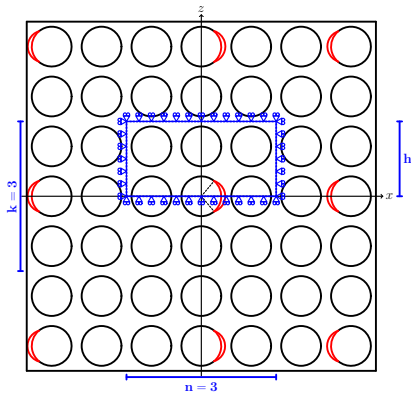


$$n \times k - H$$

$$\bar{\varepsilon}_x = \text{const}$$

$$u_x(x, h) = \bar{\varepsilon}_x x$$

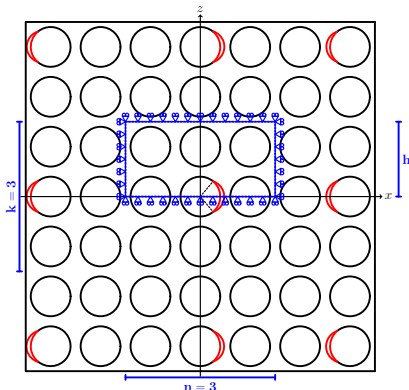
Equivalent boundary conditions: symmetric coupling



$$u_z(x, h) = \text{const}$$

$n \times k - \text{symm (coupling)}$

Equivalent boundary conditions: coupling + H



$$u_z(x, h) = \text{const}$$

$$\bar{\varepsilon}_x = \text{const}$$

$$u_x(x, h) = \bar{\varepsilon}_x x$$

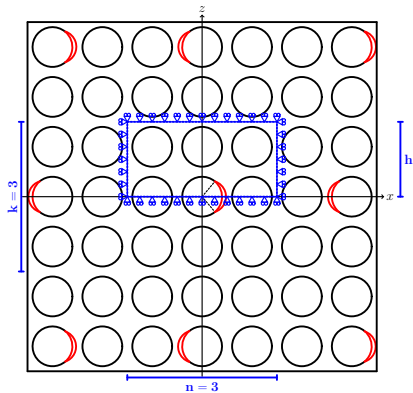
$$n \times k - \text{coupling} + H$$

Equivalent boundary conditions: anti-symmetric coupling

New set of BC!

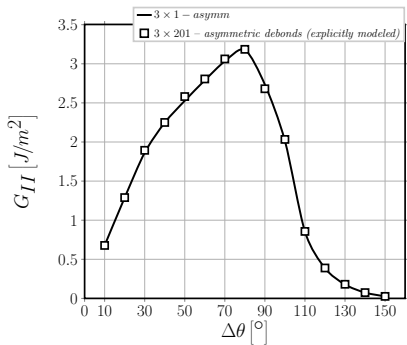
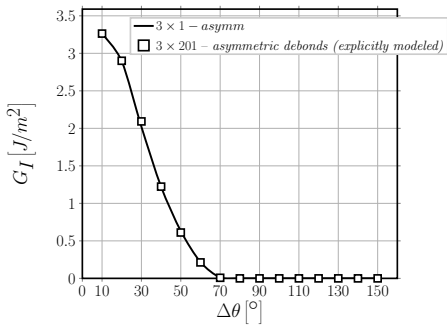
To represent debonds appearing on alternating sides along the vertical direction.

$$\begin{aligned} u_z(x, h) - u_z(0, h) &= \\ &- (u_z(-x, h) - u_z(0, h)) \\ u_x(x, h) &= -u_x(-x, h) \end{aligned}$$

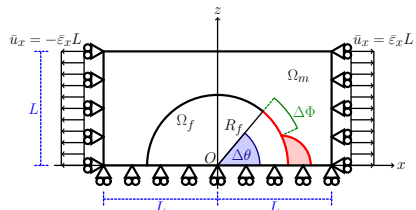


$n \times k - \text{asymm}$

Equivalent boundary conditions: anti-symmetric coupling, validation



Assumptions

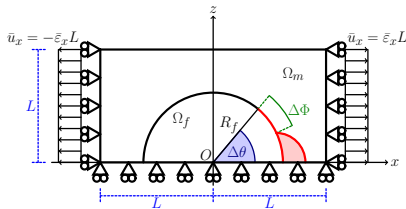


$$R_f = 1 \text{ } [\mu\text{m}] \quad L = \frac{R_f}{2} \sqrt{\frac{\pi}{V_f}}$$

- Linear elastic, homogeneous materials
- Concentric Cylinders Assembly with Self-Consistent Shear Model for UD
- Plane strain
- Frictionless contact interaction
- Symmetric w.r.t. x-axis
- Coupling of x-displacements on left and right side (repeating unit cell)
- Applied uniaxial tensile strain $\bar{\epsilon}_x = 1\%$
- $V_f = 60\%$

Material	V_f [%]	E_L [GPa]	E_T [GPa]	μ_{LT} [GPa]	ν_{LT} [-]	ν_{TT} [-]
Glass fiber	-	70.0	70.0	29.2	0.2	0.2
Epoxy	-	3.5	3.5	1.25	0.4	0.4
UD	60.0	43.442	13.714	4.315	0.273	0.465

Solution



- Compatibility conditions
- Equilibrium equations
- Non-interpenetration of crack faces
- Frictionless sliding of crack faces
- $0^\circ \leq \Delta\theta \leq 150^\circ$
- $\Delta\theta = 0^\circ \leftrightarrow$ no debond!

$\forall \Delta\theta \neq 0^\circ$

- oscillating singularity
- Mode I and Mode II SIF and ERR not defined for *open crack*
- ERR over finite distance
- FEM + LEFM (VCCT)
- receding contact

$$\frac{G(R_{f,2})}{G(R_{f,1})} = \frac{R_{f,2}}{R_{f,1}}, \frac{G(\bar{\varepsilon}_{x,2})}{G(\bar{\varepsilon}_{x,1})} = \frac{\bar{\varepsilon}_{x,2}^2}{\bar{\varepsilon}_{x,1}^2}$$

- regular mesh of quadrilaterals at the crack tip:

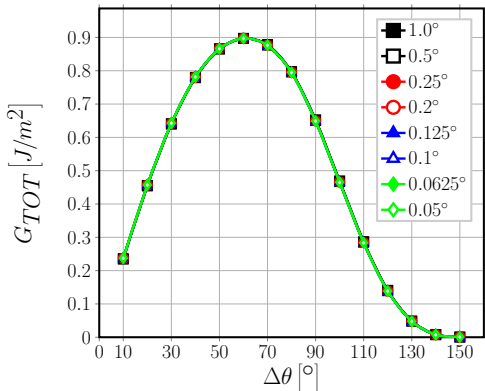
- $AR \sim 1, \quad \delta = 0.05^\circ$

$\forall \Delta\theta$

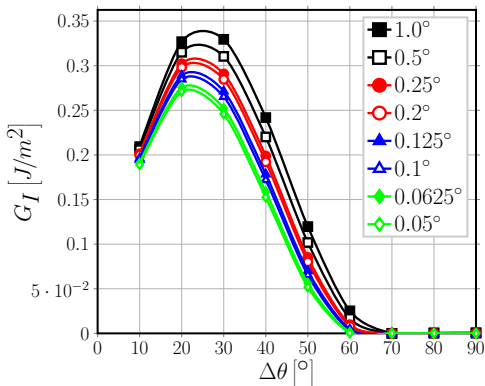
- 2nd order shape functions

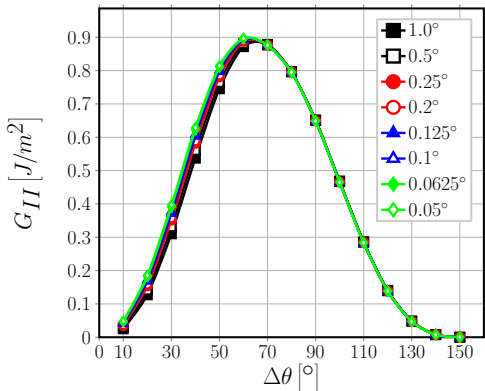
Introduction Modeling Convergence Debond Initiation Debond Propagation Moving Forward
 G_{TOT} G_I G_{II} Vectorial formulation of VCCT Asymptotic behavior Numerical convergence Observations δ selection

CONVERGENCE

G_{TOT} 

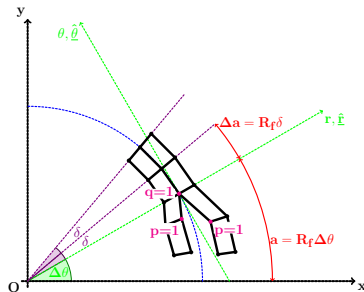
$\rightarrow 1 \times 1 - free, V_f = 0.1\%, 2^{nd} order elements$

G_I  $\rightarrow 1 \times 1 - free, V_f = 0.1\%, 2^{nd} \text{ order elements}$

G_{II} 

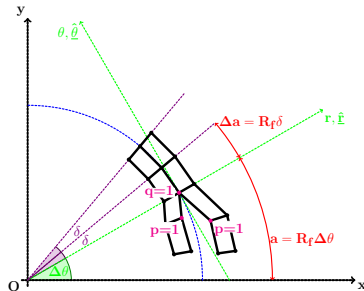
$\rightarrow 1 \times 1 - free, V_f = 0.1\%, 2^{nd} \text{ order elements}$

Vectorial formulation of VCCT



$$\begin{aligned}
 G_{TOT} = & \frac{1}{2R_f\delta} \sum_{p=1}^{m+1} \sum_{q=1}^{m+1} \text{Tr} \left(Q \underline{\underline{R}}_{\underline{\underline{\delta}}=\Delta\theta} \underline{\underline{K}}_{xy,q} \underline{u}_{xy,q}^T \underline{\underline{u}}_{xy,p} \underline{\underline{R}}_{\underline{\underline{\delta}}=\Delta\theta}^T \underline{\underline{P}}_{\underline{\underline{\delta}}=\delta}^T \underline{\underline{T}}_{pq}^T \right) + \\
 & + \frac{1}{2R_f\delta} \sum_{p=1}^{m+1} \sum_{q=1}^{m+1} \text{Tr} \left(Q \underline{\underline{R}}_{\underline{\underline{\delta}}=\Delta\theta} \widetilde{\underline{\underline{F}}}_{xy,q} \underline{u}_{xy,p}^T \underline{\underline{R}}_{\underline{\underline{\delta}}=\Delta\theta}^T \underline{\underline{P}}_{\underline{\underline{\delta}}=\delta}^T \underline{\underline{T}}_{pq}^T \right)
 \end{aligned}$$

Vectorial formulation of VCCT



$$\begin{aligned} \underline{G} = \begin{bmatrix} G_I \\ G_{II} \end{bmatrix} &= \frac{1}{2R_f\delta} \sum_{p=1}^{m+1} \sum_{q=1}^{m+1} \text{Diag} \left(Q_{\underline{\delta}=\Delta\theta} R_{\underline{\Delta\theta}=\underline{\delta}} K_{\underline{x}_{xy},q} u_{xy,q}^T R_{\underline{\Delta\theta}=\underline{\delta}}^T P_{\underline{\delta}=pq}^T T^T \right) + \\ &+ \frac{1}{2R_f\delta} \sum_{p=1}^{m+1} \sum_{q=1}^{m+1} \text{Diag} \left(Q_{\underline{\delta}=\Delta\theta} R_{\underline{\Delta\theta}=\underline{\delta}} \tilde{K}_{N,q} u_N^T u_{xy,p}^T R_{\underline{\Delta\theta}=\underline{\delta}}^T P_{\underline{\delta}=pq}^T T^T \right) \end{aligned}$$

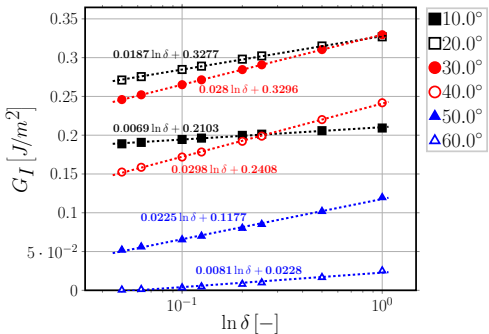
Asymptotic behavior

$$\frac{\partial \underline{G}}{\partial \delta} = \frac{1}{\delta} \underline{G} + \frac{1}{2R_f \delta} (\dots)$$

$$u(\delta) \sim \sqrt{\delta} (\sin, \cos)(\epsilon \log \delta) \quad \text{with} \quad \epsilon = \frac{1}{2\pi} \log \left(\frac{1-\beta}{1+\beta} \right)$$

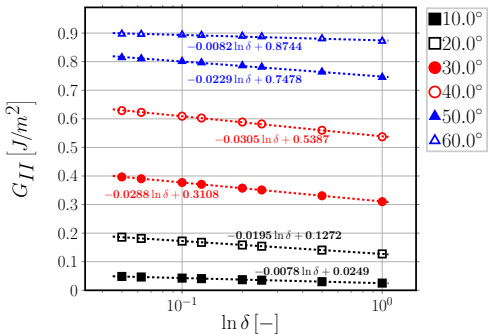
$$\lim_{\delta \rightarrow 0} \frac{\partial \underline{G}}{\partial \delta} \sim \frac{1}{\delta} \xrightarrow{\int d\delta} \lim_{\delta \rightarrow 0} \underline{G} \sim \underline{A} \log(\delta) + \underline{B}.$$

Numerical convergence: G_I



$\rightarrow 1 \times 1 - free, V_f = 0.1\%, 2^{nd} order elements$

Numerical convergence: G_{II}



$\rightarrow 1 \times 1 - free, V_f = 0.1\%, 2^{nd} \text{ order elements}$

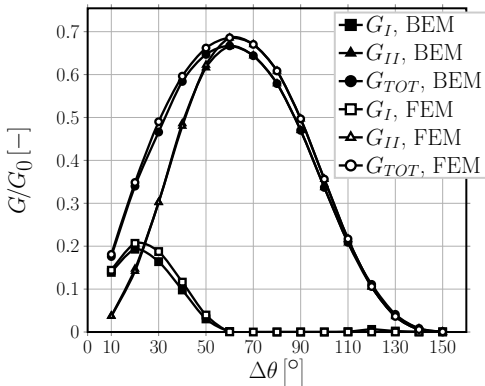
Observations

- Total ERR does not depend on element size at the crack tip in any configuration of the crack.
- For the *close crack*, Mode II ERR does not depend on element size, as it is equal to the total ERR.
- For the *open crack*, Mode I and Mode II ERR depend logarithmically on element size.
- For the *open crack*, Mode I and Mode II ERR are not bounded.

It seems reasonable to conclude that...

...a criterion based on the reduction of the error between successive iterations is inadequate to identify the optimal element size. The FEM model has to be validated with respect to external data (experimental, analytical or numerical from a different method).

δ selection

París et al., J. Appl. Mech. **74** (4), 2007.Sandino et al., Eng. Fract. Mech. **168**, 2016. $\rightarrow 1 \times 1 - free, V_f = 0.01\%, 2^{nd} \text{ order elements}, \delta = 0.05^\circ$

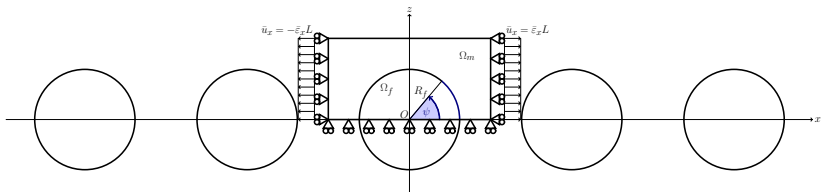
Introduction Modeling Convergence Debond Initiation Debond Propagation Moving Forward

Analysis of initiation: main features Stress profiles in the matrix at the interface Observations

DEBOND INITIATION

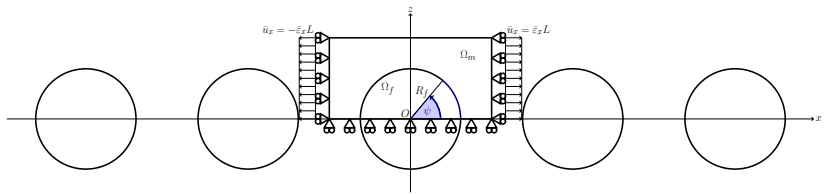
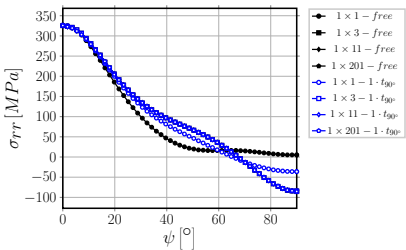
Analysis of initiation: main features

NO DEBOND!

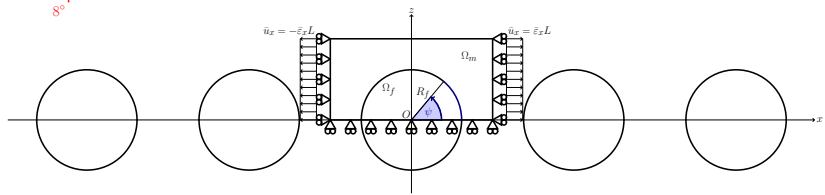
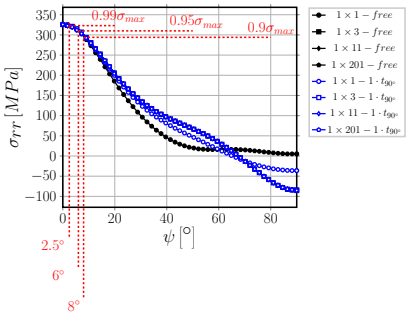


- No stress-based initiation criterion is assumed
- Profiles of stresses in the matrix at the interface are analyzed
- Where does the maximum occur? How fast does the stress decrease from the peak value?
- Effect of thickness of UD/90° ply? Effect of the presence of 0° ply?

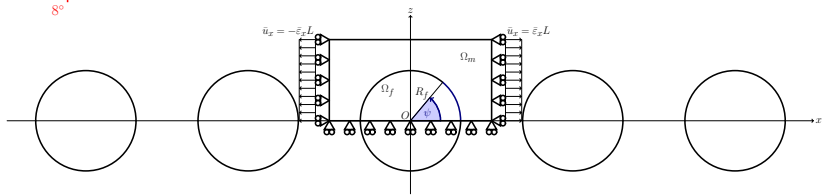
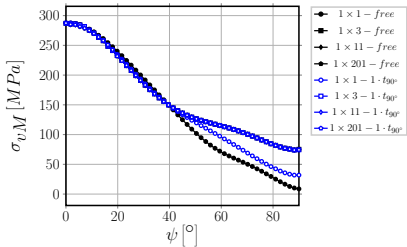
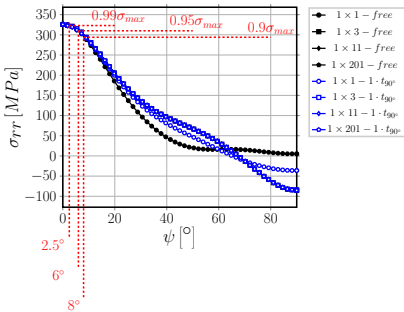
Stress profiles in the matrix at the interface



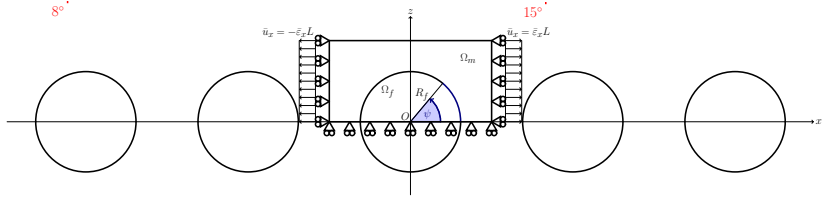
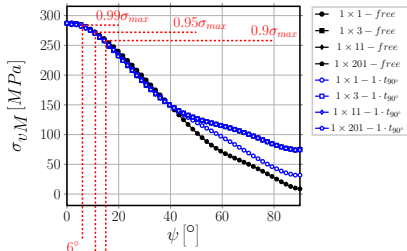
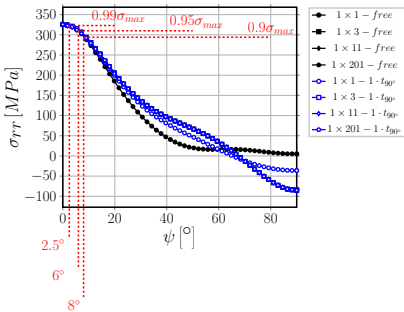
Stress profiles in the matrix at the interface



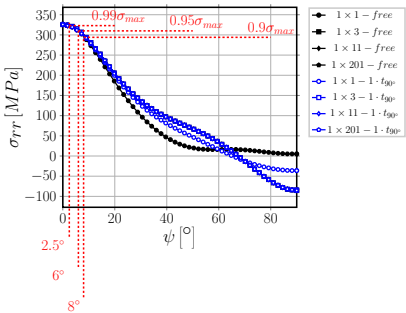
Stress profiles in the matrix at the interface



Stress profiles in the matrix at the interface



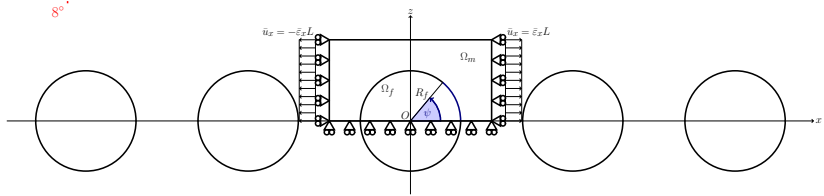
Stress profiles in the matrix at the interface



Similar results for:

$$\sigma_{LHS,2D} - \sigma_{LHS,3D}$$

$$\sigma_{LMPS,2D} - \sigma_{LMPS,3D}$$



Observations

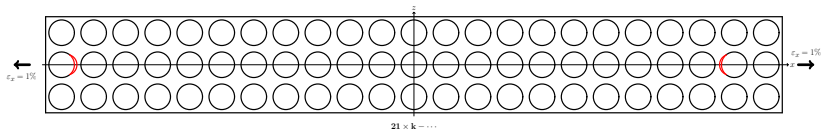
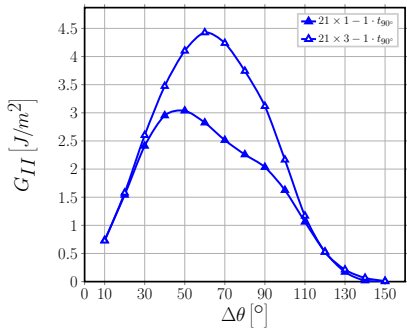
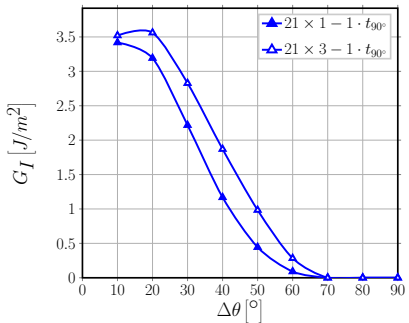
- For all stresses analyzed, no significant difference is present between the different RUCs for $\psi \leq 10^\circ$;
- for all stresses analyzed, no difference can be observed by increasing k when $k \geq 3$;
- for all stresses analyzed, no difference can be observed between $1 \times k - \text{free}$ and $1 \times k - 1 \cdot t_{90^\circ}$ for $k \geq 3$;
- σ_{rr} , $\sigma_{LHS,2D}$, $\sigma_{LHS,3D}$, $\sigma_{vM,2D}$, $\sigma_{LMPS,2D}$ and $\sigma_{LMPS,3D}$ all reach their peak value at 0° and 180° and decrease to 99% the peak value between 2° and 8° , to 95% the peak value between 6° and 12° and to 90% the peak value between 8° and 15° from the occurrence of the maximum.

It seems reasonable to conclude that...

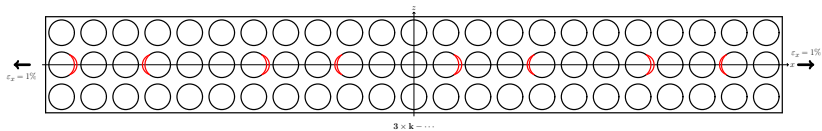
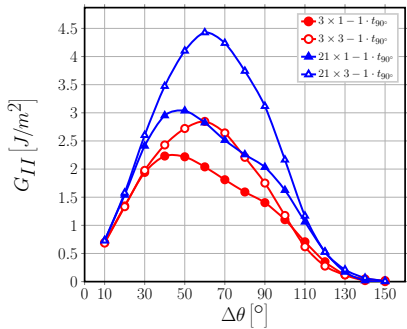
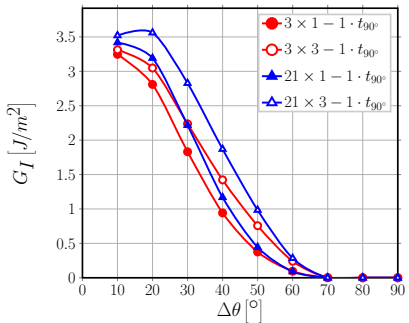
...a stress-based criterion would predict, irrespectively of the specific criterion chosen, the onset of an interface crack at 0° or 180° with an initial size at least comprised in the range $2^\circ - 8^\circ$ (1% margin) and likely in the range $6^\circ - 12^\circ$ (5% margin). Thus, no evident effect of 90° or 0° layer thickness can be observed.

DEBOND PROPAGATION

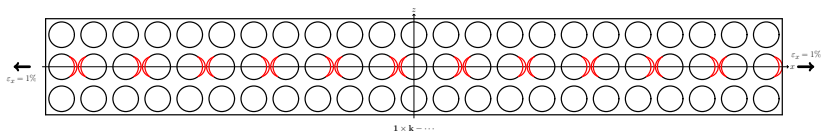
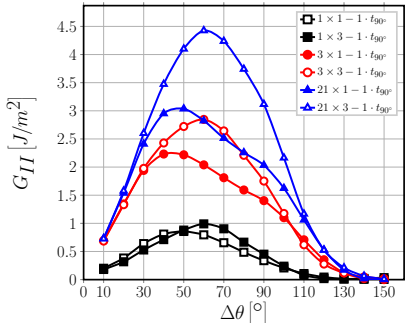
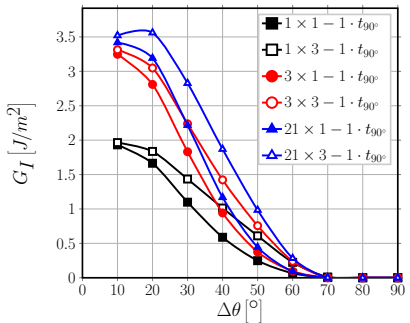
Interaction of Debonds: Crack Shielding



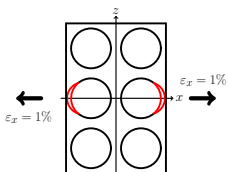
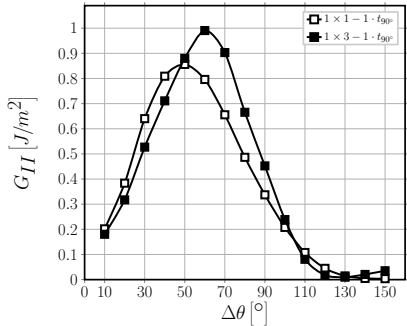
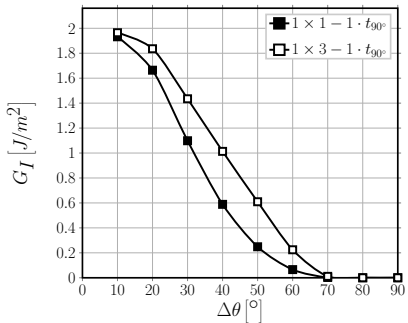
Interaction of Debonds: Crack Shielding



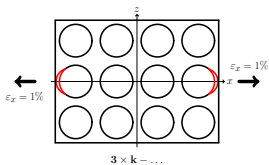
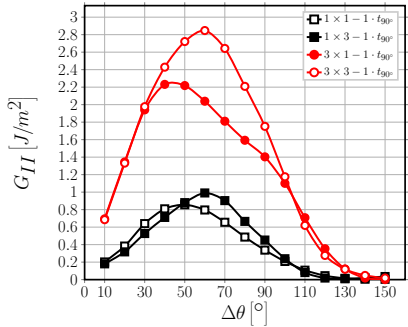
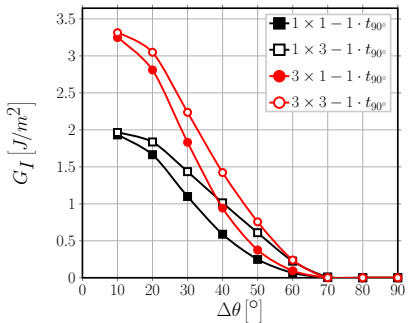
Interaction of Debonds: Crack Shielding



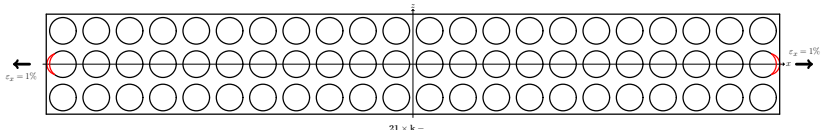
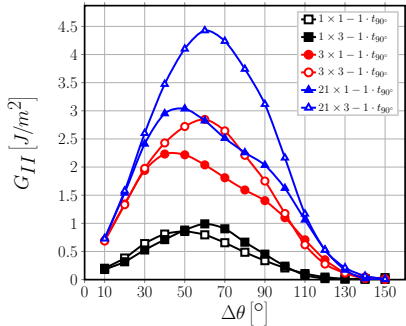
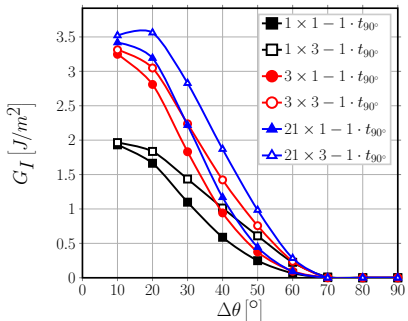
Interaction of Debonds: Strain Magnification



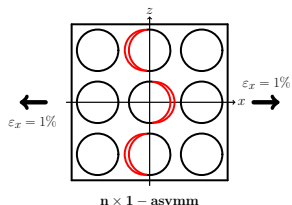
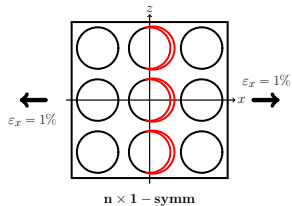
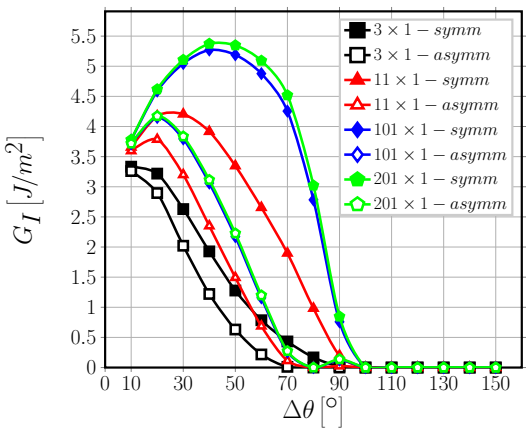
Interaction of Debonds: Strain Magnification



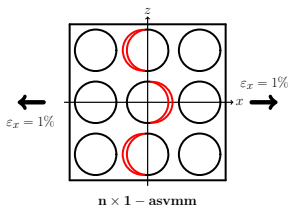
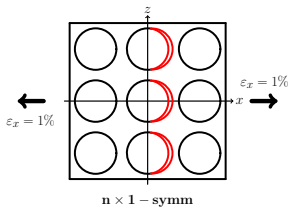
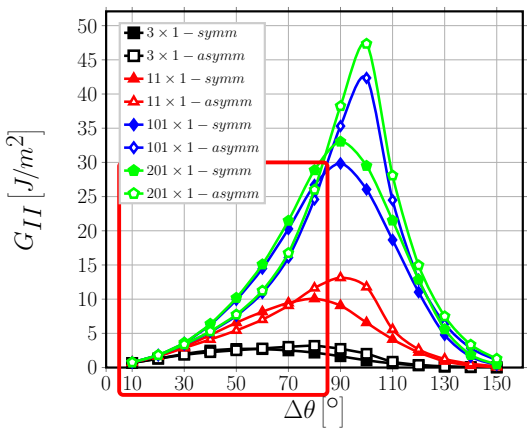
Interaction of Debonds: Strain Magnification



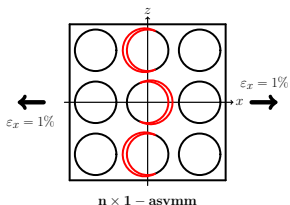
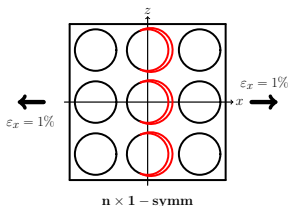
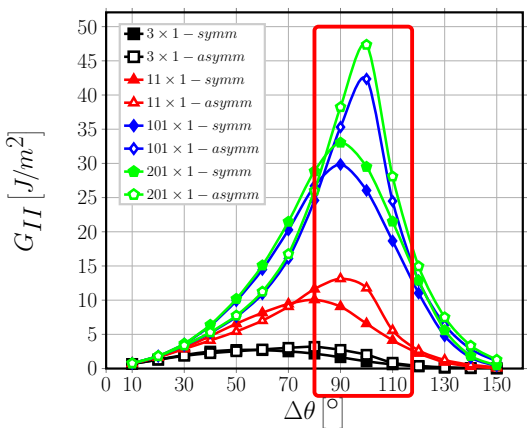
Consecutive Debonds: Mode I



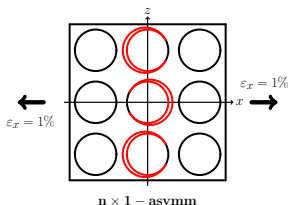
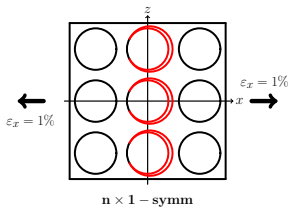
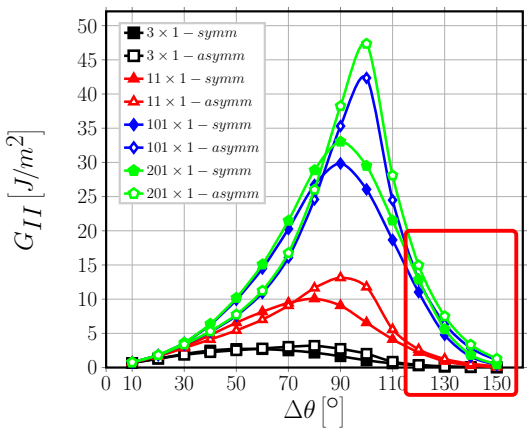
Consecutive Debonds: Mode II



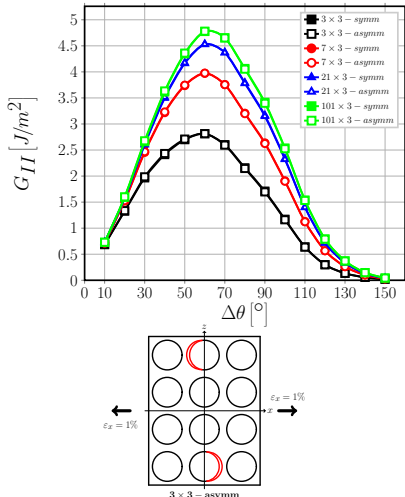
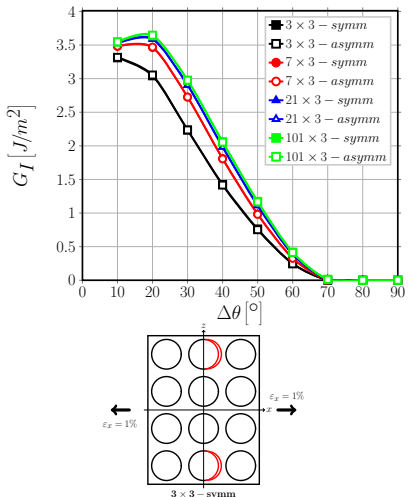
Consecutive Debonds: Mode II



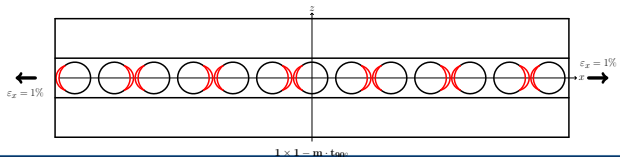
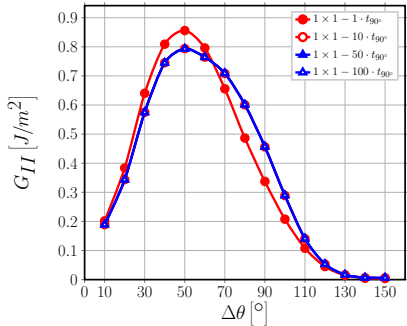
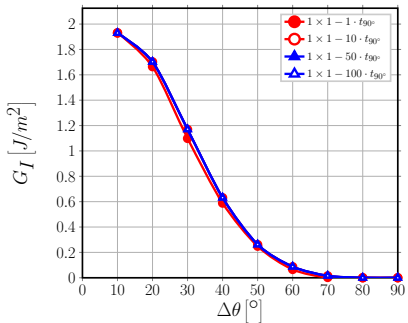
Consecutive Debonds: Mode II



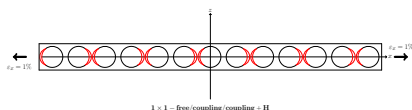
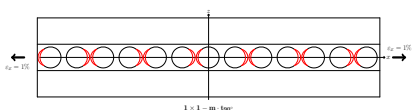
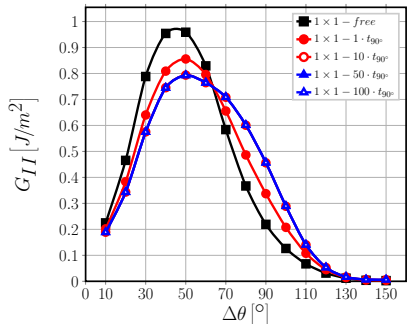
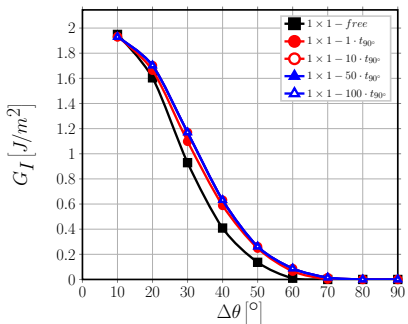
Non-Consecutive Debonds



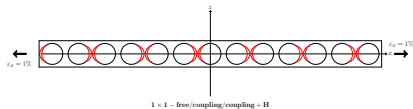
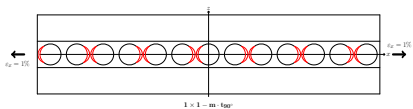
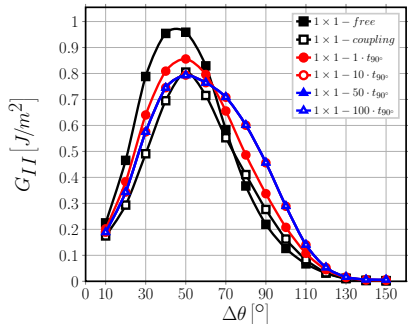
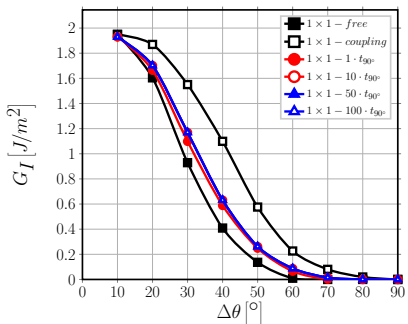
Effect of 0° ply thickness



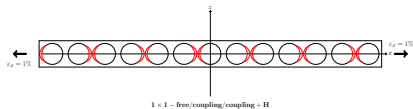
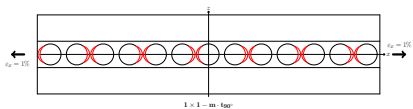
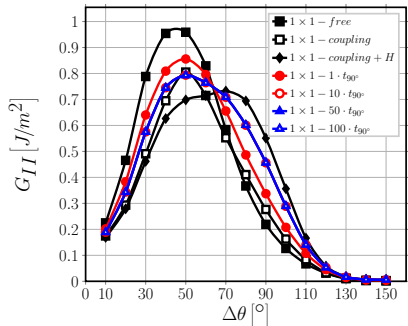
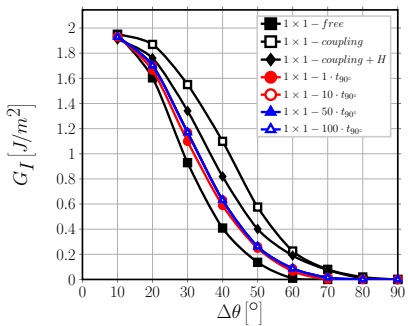
Effect of 0° ply thickness



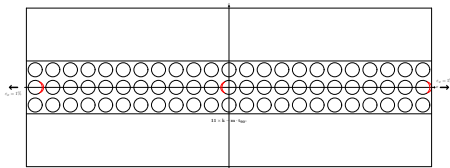
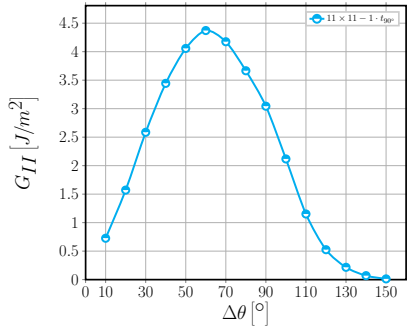
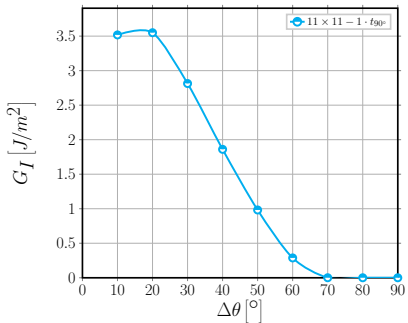
Effect of 0° ply thickness



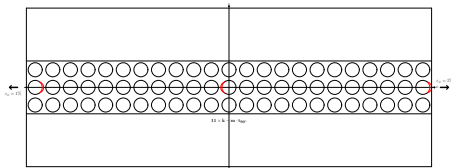
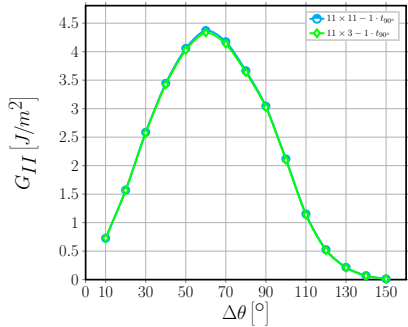
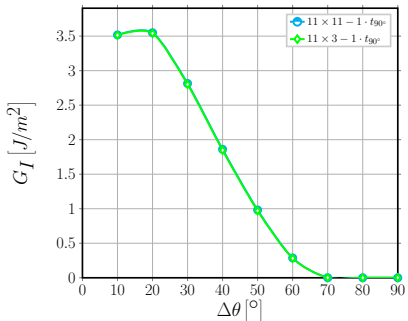
Effect of 0° ply thickness



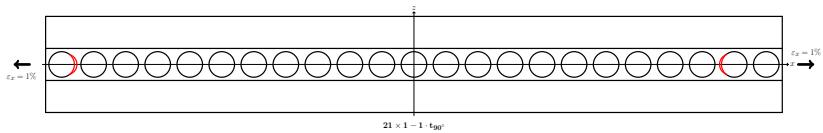
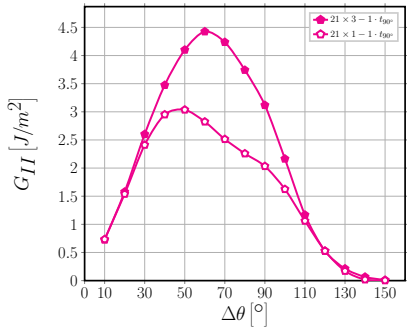
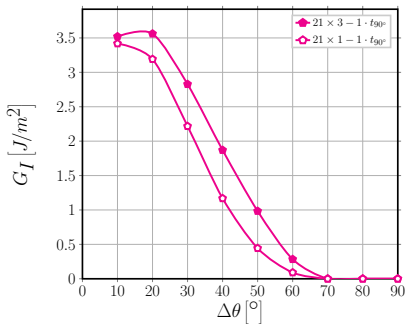
Effect of 90° ply thickness



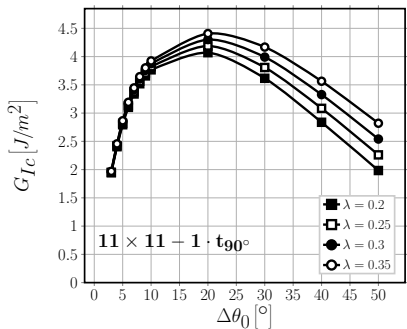
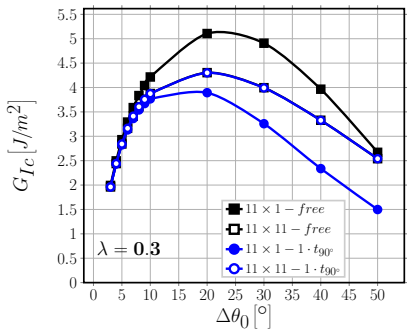
Effect of 90° ply thickness



Effect of 90° ply thickness



Estimation of G_{Ic}

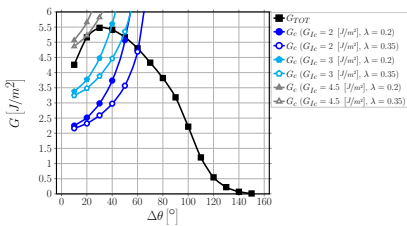


$$G_{Ic} = \frac{G_c}{1 + \tan^2((1 - \lambda) \Psi_G)} \Big|_{G_c=G_{TOT}(\Delta\theta_0)}, \quad \Psi_G = \tan^{-1} \left(\sqrt{\frac{G_{II}}{G_I}} \right) \Big|_{\Delta\theta_0}$$

$G_{Ic} \in [2, 4.5] \text{ J/m}^2$ with $R_f = 1 \mu\text{m}$, $\bar{\varepsilon}_x = 1\%$, $G_{Ic} \in [3.2, 7.2] \text{ J/m}^2$ with $R_f = 10 \mu\text{m}$, $\bar{\varepsilon}_x = 0.4\%$

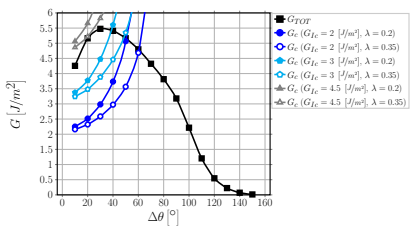
Estimation of $\Delta\theta_{max}$

$21 \times 21 - \text{free}$



$$\Delta\theta_{max} \in (40^\circ - 60^\circ)$$

$21 \times 21 - 1 \cdot t_{90^\circ}$



$$\Delta\theta_{max} \in (40^\circ - 60^\circ)$$

$$G_{TOT}(\Delta\theta) > G_c = G_{lc} \left(1 + \tan^2((1-\lambda)\Psi_G) \right), \quad \Psi_G = \tan^{-1} \left(\sqrt{\frac{G_{II}}{G_I}} \right) \Big|_{\Delta\theta}$$

Estimation of $\Delta\theta_{max}$

Estimated debond size range in cross-ply ($n \times k - 1 \cdot t_{90^\circ}$)

$40^\circ - 60^\circ$

Measured debond size range in cross-ply (Correa et al., Compos. Sci. Technol. 155 (213-220), 2018)

$21.4^\circ - 89.2^\circ$, average 49.3° , standard deviation of 11.7°

63% of measurements in $40^\circ - 60^\circ$ range

Observations

- No significant effect of the 90° layer thickness has been observed.
- No significant effect of the 0° layer thickness has been observed.
- Only in the case of a 1-fiber-row 90° layer the presence of the 0° layer results in a sizeable effect on debond ERR.
- Debond-debond interaction along the vertical direction has significant influence on ERR, but the presence of just 2 fully bonded fibers in between drastically reduce its importance.

It seems reasonable to conclude that...

...debond ERR, and thus debond propagation, is affected by changes in the microstructure only in a very small neighborhood, $\sim 1 - 2 \phi_{fiber}$ around the debond itself.

 **MOVING FORWARD**

Moving Forward: Ideas

- ▶ Microscopic characterization of transverse cracks, debonds and microstructure: optical microscope and image analysis, edge view (both sides), increasing load levels on same specimen, different lay-ups and materials
 - SEM? TEM? μ -CT?
- ▶ Microstructure-controlled debonding as toughening mechanisms for thin-ply laminates
 - 3D-printing? Improved spread-tow technique?

Thank you for listening today!



LULEÅ
UNIVERSITY
OF TECHNOLOGY



Education and Culture

Erasmus Mundus